Mixed Oxidation State Confacial Bioctahedral Complexes of Tungsten Possessing Strong Metal–Metal Interactions. Part 2.† Synthesis, *X*-Ray Crystal Structure and Electron Spin Resonance Studies of the W^{III}/W^{IV} Complex $[AsPh_4]_2[Cl_3W(\mu\text{-}Cl)(\mu\text{-}SPh)_2WCl_3]\cdot 1.4CH_2Cl_2$ ‡

Joanne M. Ball, P. Michael Boorman,* Kelly J. Moynihan, Vikram D. Patel, and John F. Richardson
Department of Chemistry, University of Calgary, Calgary, Alberta, Canada T2N 1N4
David Collison and Frank E. Mabbs *
Department of Chemistry, University of Manchester, Manchester M13 9PL

The mixed oxidation state dimeric tungsten(III/IV) species $[(Me_2S)Cl_2W(\mu\text{-}Cl)(\mu\text{-}SPh)_2WCl_2(SMe_2)]$ and $[Cl_3W(\mu\text{-}Cl)(\mu\text{-}SPh)_2WCl_3]^{2-}$ have been synthesized. A single-crystal *X*-ray diffraction study of the compound $[AsPh_4]_2[Cl_3W(\mu\text{-}Cl)(\mu\text{-}SPh)_2WCl_3]\cdot 1.4CH_2Cl_2$ (1) shows that the two tungsten atoms have identical environments, imposed by a crystallographic two-fold axis passing through the bridging chlorine atom. Structural parameters indicate a strong tungsten–tungsten bond of length 2.519(2) Å, in a distorted confacial bioctahedral structure. Crystals are monoclinic, space group *C*2/*c*, with unit-cell dimensions (at 296 K) a = 22.584(15), b = 12.174(4), c = 24.359(15) Å, β = 104.15(3)°, and Z = 4. The structure was refined to R = 0.072 (R' = 0.096) for 3 327 unique reflections. E.s.r. spectra of (1) as a powdered solid at 77 and 298 K and as a frozen solution in CH_2Cl_2 at 77 K were obtained at *X*-band frequencies. The spectra have been interpreted as a rhombic $S = \frac{1}{2}$ system, and have been simulated on this basis. The spectra are characterized by a large anisotropy in the g values, with one g value considerably greater than 2.

Numerous simple (*i.e.* non-chelating type) ligand-bridged dinuclear complexes of molybdenum and tungsten have been prepared and characterized in the past 15 years,[1] but relatively few species of this sort, in which the metal centres possess different formal oxidation states, have been studied.[2] Thus, of the many physical techniques accessible for studying the electronic structures of bridged dimeric complexes, the use of e.s.r. spectroscopy has usually been precluded. The mixed-valent (W^{III}/W^{IV}) $W_2Br_9^{2-}$ ion has been reported,[3] but no e.s.r. spectral data were presented. The W^{III}/W^{IV} complex $[(Me_2S)Cl_2W(\mu\text{-}SEt)_3WCl_2(SMe_2)]$ was recently synthesized and characterized in our laboratories,[4] but only an ill resolved e.s.r. spectrum was obtained (g = 2.00) for this compound, even at 77 K. Consistent with the lack of a well resolved e.s.r. spectrum, this complex exhibits a sharp ^1H n.m.r. spectrum, even at room temperature.[5] The potential of e.s.r. spectroscopy for studying the electronic structures of dinuclear complexes which do or do not contain metal–metal bonds has been clearly demonstrated recently. In a series of papers discussing the e.s.r. properties of strongly metal–metal bonded species such as $M_2Cl_8^{3-}$ (M = Tc, Re, or Mo), $[M_2(O_2CPr^n)_4]^+$ (M = Ru or Mo), and $[Mo_2(SO_4)_4]^{3-}$, Cotton and Pedersen [6–10] were able to show that, in most cases, the odd electron was delocalized over both metal atoms.[6–10] In none of these cases, however, was the structure of the mixed-valent dimeric anion of the confacial bioctahedral type. Conversely, Stephenson and co-workers [11,12] have studied electrochemically generated Ru^{II}/Ru^{III} dimers with confacial bioctahedral frameworks which do not contain metal–metal bonds. Their e.s.r. studies of these complexes confirmed the presence of isolated valences.

We now report on the second in a series of mixed oxidation state (M^{III}/M^{IV}) confacial bioctahedral complexes of tungsten or molybdenum which possess strong metal–metal interactions and which are e.s.r. active. The metal ions in these complexes have identical environments and being metal–metal bonded, they could be termed type IIIA according to the Robin and Day classification scheme of mixed-valent complexes.[13] The theoretical study of Summerville and Hoffmann [14] dealing with M_2L_9 species showed that there is considerable mixing of ligand (L) and metal orbitals in the bridging region. Thus, in the triply bridged complexes of the type reported here, it is anticipated that, by a judicious selection of metal and bridging ligand, experimental insight into the electronic structure of this type of complex could be realised. Herein, we report the synthesis, *X*-ray crystal structure, and e.s.r. data for the compound $[AsPh_4]_2[Cl_3W(\mu\text{-}Cl)(\mu\text{-}SPh)_2WCl_3]\cdot 1.4CH_2Cl_2$ (1).

Experimental

General Procedures.—All manipulations were carried out in a dry nitrogen-filled glove-box or on a standard double manifold. Analytical grade solvents were dried (CH_2Cl_2 over P_4O_{10}, hexane over CaH_2) and freshly distilled under an atmosphere of dry nitrogen immediately before use. Methyl sulphide (Aldrich Chemicals) was dried over calcium hydride and distilled under nitrogen before use. The compound $[WCl_4(SMe_2)_2]$ (2) was prepared by refluxing WCl_4 with the neat ligand in an evacuated, sealed Pyrex tube, as previously described.[15] Phenylthiotrimethylsilane was synthesised from $[\{Pb(SPh)_2\}_n]$ (Aldrich) by the published procedure.[16] $AsPh_4Cl$ was obtained as the hydrate (Alfa Products) and was dehydrated by heating under vacuum for 16 h at 385 K. Tungsten was analyzed by ignition to the oxide (WO_3) in a silica crucible after prior digestion with nitric acid. All other

---

† Part 1 is ref. 4.

‡ Bis(tetraphenylarsonium) μ-chloro-hexachloro-bis(μ-phenylthiolato)-ditungstate(III/IV)(*W*–*W*).

Supplementary data available (No. SUP 23684, 34 pp.): observed and calculated structure factors, anion anisotropic thermal parameters, cation and solvent positional, structural, and anisotropic thermal parameters, calculated H-atom parameters. See Notices to Authors, No. 7, *J. Chem. Soc., Dalton Trans.*, 1981, Index issue.

analyses were obtained commercially (Galbraith Laboratories Inc., Knoxville, Tennessee).

Synthesis.—The compound $[AsPh_4]_2[Cl_3W(\mu\text{-}Cl)(\mu\text{-}SPh)_2WCl_3]\cdot 1.4CH_2Cl_2$ (1) was prepared in a two-step process from $[WCl_4(SMe_2)_2]$ (2). The exact calculated one mol equiv. of $SiMe_3(SPh)$, dissolved in CH_2Cl_2, was added to a stirred solution of (2) (1.71 g, 3.8 mmol) in CH_2Cl_2 (*ca.* 30 cm^3). The colour changed instantaneously from clear orange-red to an opaque red-brown. After stirring for 15 h at ambient temperature, the reaction mixture was filtered and the rust-coloured microcrystalline precipitate that remained on the frit was washed with hexane (2 × 20 cm^3) and dried *in vacuo* (yield *ca.* 0.5 g). Spectroscopic (see below) and elemental analyses of this material and the nature of its chloroanionic derivative (1) (see below) indicate that this compound is $[(Me_2S)Cl_2W(\mu\text{-}Cl)(\mu\text{-}SPh)_2WCl_2(SMe_2)]$ (3) (Found: C, 21.5; H, 2.5; Cl, 22.5; S, 14.1; W, 41.2. Calc. for $C_{16}H_{22}Cl_5S_4W_2$: C, 21.65; H, 2.5; Cl, 19.95; S, 14.45; W, 41.45%). I.r. data (2 000—250 cm^{-1}, Nujol mull, CsI plates, Perkin-Elmer 467 spectrophotometer): 1 570w, 1 410m, 1 325w, 1 180w, 1 031w, 1 020m, 995w, 980m, 830vw, 740vs ν(C–S), 685m ν(C–S), 678s ν(C–S), 470m, 350s ν(W–Cl), 331vs ν(W–Cl), 309s ν(W–Cl), and 275m cm^{-1} ν(W–Cl). U.v.–visible absorption data (250—850 nm, CH_2Cl_2 solution, Cary 219 spectrophotometer, 10-mm matched quartz cells): 496 (ε = 1 000), 422 (ε = 940), and 340 nm (ε = 2 100 dm^3 mol^{-1} cm^{-1}). The band at 340 nm is in fact a shoulder of an intense charge-transfer band in the u.v. region. N.m.r. data are presented and discussed later.

Compound (3) is very air sensitive and must be handled at all times in an inert atmosphere. It is slightly soluble in CH_2Cl_2, $C_2H_4Cl_2$ and $C_2H_2Cl_4$ to give very air sensitive reddish solutions.

Since compound (3) could not be obtained in a crystalline form suitable for *X*-ray diffraction studies, the labile terminal SMe_2 ligands were displaced by Cl^- (using $AsPh_4Cl$) in CH_2Cl_2 to form the more stable compound (1). Tetraphenylarsonium chloride (0.45 g, 1.08 mmol) was added to a stirred solution of (3) (0.48 g, 0.54 mmol) in CH_2Cl_2 (*ca.* 40 cm^3). A subtle colour change occurred, and the mixture was allowed to stir for 15 h at ambient temperature. The reaction solution was then filtered, yielding a clear orange-red filtrate to which hexane (*ca.* 10 cm^3) was slowly added. Well formed burgundy crystals of (1) which were suitable for *X*-ray crystallographic measurements grew from this solution at *ca.* 250 K over a period of 3 d. *X*-Ray crystallographic data (see below) has unequivocally established that (1) is $[AsPh_4]_2[Cl_3W(\mu\text{-}Cl)(\mu\text{-}SPh)_2WCl_3]\cdot 1.4CH_2Cl_2$. The i.r. spectrum of (1) is dominated by bands due to $AsPh_4^+$ and hence no i.r. data are given here. The 200-MHz ^{1}H n.m.r. spectrum (ambient temperature, Varian XL-200 FT spectrometer, $C_2D_2Cl_4$ solution) consists of a collection of broad, poorly defined resonances in the range δ 7—8 p.p.m., assignable to the phenyl ring protons of the cations, and a singlet at δ 5.25 p.p.m. corresponding to the CH_2Cl_2 solvate molecules (integration ratio *ca.* 20 : 1). U.v.–visible absorption data (250—850 nm, CH_3CN solution): 486 (ε = 2 560), 437 (ε = 2 980), and 379 nm (ε = 2 240 dm^3 mol^{-1} cm^{-1}). An intense absorption (ε > 7 000 dm^3 mol^{-1} cm^{-1}) which tails into the visible region is also present in the u.v. region of the absorption spectrum ($\leqslant$ 325 nm).

In the solid state (1) can be handled in air for several hours, but it is best stored for prolonged periods under a CH_2Cl_2-saturated nitrogen atmosphere. The complex (1) is slightly soluble in CH_2Cl_2, $C_2H_4Cl_2$, $C_2H_2Cl_4$, and CH_3CN, giving orange solutions which are slightly air sensitive.

X-Ray Crystal Structure of $[AsPh_4]_2[Cl_3W(\mu\text{-}Cl)(\mu\text{-}SPh)_2WCl_3]\cdot 1.4CH_2Cl_2$.—*Collection and reduction of the data.* Preliminary photographic examination and observed extinctions during data collection [(*h k l*), $h + k = 2n + 1$; (*h* 0 *l*), $l = 2n + 1$] identified the space group as either *Cc* or *C*2/*c*. The choice of *C*2/*c* was later substantiated by the centric distribution of *E* values. With four formula units per unit cell, site symmetry 2 is imposed on the anion.

An epoxy-coated crystal of (1) having dimensions *ca.* 0.36 × 0.31 × 0.06 mm was mounted in an arbitrary orientation on an Enraf-Nonius CAD-4F automated diffractometer. The final unit-cell parameters were obtained by least-squares refinement of the setting angles for 20 accurately centred reflections having $18 < \theta < 23°$.

Crystal data. $C_{60}H_{50}As_2Cl_7S_2W_2\cdot 1.4CH_2Cl_2$, M = 1 717.8, Monoclinic, space group *C*2/*c*, a = 22.584(15), b = 12.174(4), c = 24.359(15) Å, β = 104.15(3)°, U = 6 494(6) Å^3, Z = 4, D_c = 1.76 g cm^{-3}, $F(000)$ = 3 336, graphite-monochromated Mo-K_α radiation, λ = 0.710 69 Å, μ(Mo-K_α) = 52.9 cm^{-1}.

Intensity data were collected at room temperature [296(3) K] using the ω—2θ scan mode with a width of $\Delta\omega = 1.5\ (0.55 + 0.35\ \tan\theta)°$. The intensity was calculated as $I = [P - 2(B1 + B2)]Q$ where P is the sum of the central 64 steps of a 96-step scan, Q is the scan rate, and $B1$ and $B2$ are the backgrounds. The standard deviation of the intensity $\sigma(I) = [P + 4(B1 + B2)]^{\frac{1}{2}}Q$. Three standard reflections (−9, −5, 1; 0, 0, 12; 6, 4, 0) were measured every 1 000 s of exposure time during data collection as a check on crystal quality. The intensities of these standards did not change significantly during the acquisition period. 5 744 Unique reflections were measured to a maximum 2θ = 50°, and of these, 3 327 were considered observed with $I > 3\sigma(I)$. The data were corrected for background, Lorentz, and polarization effects and *E* values were calculated using a *K* curve.* The data crystal was carefully measured using a microscope fitted with a filar eyepiece to permit an absorption correction. The crystal possessed nine faces, namely {100}, {001}, (1−10), (−110), (−101), (111), and (1 − 11) as determined by optical goniometry. An absorption correction † showed minimum and maximum correction factors of 1.68 and 6.82 respectively.

Solution and refinement of the structure. Atomic scattering factors were those of Cromer and Mann.[17] Real and anomalous dispersion corrections were applied to all non-hydrogen atoms.[18] The position of the unique W atom was readily obtained from a three-dimensional Patterson synthesis. A series of difference-Fourier syntheses revealed the location of all remaining non-hydrogen atoms. The crystallographically imposed two-fold axis passes through the bridging Cl [Cl(1)] and bisects the W–W vector of the anion.

The structure was refined by full-matrix least-squares techniques based on *F*. In the latter cycles, all non-hydrogen atoms were refined with anisotropic thermal parameters. The 27 unique H atoms of the structure were included in idealized positions (C–H = 0.95 Å for sp^2 C, C–H = 1.00 Å for sp^3 C) with thermal parameters set to 10% greater than the C atom to which they are attached, but not refined. The occupancy factor of the CH_2Cl_2 solvate was refined and found to be approximately 0.7. The value was set to 0.7 in the final cycles. This deviation from unity is probably a result of solvent loss during storage of the crystals in a dry-box prior to data

---

* Computing was performed at the University of Calgary using the *X*-RAY 76 package of crystallographic programs, Technical Report TR-446, ed. J. M. Stewart, Computer Science Center, University of Maryland.

† The absorption correction was done using the program CADABS, a local modification of a program by P. Coppens *et al.*, Crystallographic Computing Programs, State University of New York at Buffalo.

Table 1. Positional parameters[a] (× 10^4) of the unique, non-hydrogen atoms of the anion $[Cl_3W(\mu\text{-}Cl)(\mu\text{-}SPh)_2WCl_3]^{2-}$

Atom	*X*/*a*	*Y*/*b*	*Z*/*c*
W	−49.5(4)	2 352.5(5)	1 973.7(3)
S	811(2)	3 222(4)	2 624(2)
Cl(1)	0[b]	637(5)	2 500[b]
Cl(2)	628(3)	1 513(5)	1 474(3)
Cl(3)	−874(3)	1 587(5)	1 266(2)
Cl(4)	−81(3)	3 986(4)	1 428(2)
C(11)	1 531(10)	2 574(17)	2 756(9)
C(12)	2 024(10)	3 269(18)	2 908(10)
C(13)	2 612(11)	2 893(22)	3 023(11)
C(14)	2 711(12)	1 762(30)	2 976(12)
C(15)	2 224(14)	1 055(24)	2 808(12)
C(16)	1 657(11)	1 475(21)	2 722(11)

[a] Estimated standard deviations in this and other Tables are given in parentheses. [b] Parameters are restricted by the symmetry of the crystal.

Table 2. Selected bond lengths (Å) and angles (°) in the anion $[Cl_3W(\mu\text{-}Cl)(\mu\text{-}SPh)_2WCl_3]^{2-}$

(*a*) Bond lengths			
W–W′	2.519(2)	W–Cl(1)	2.439(6)
W–S	2.429(5)	W–Cl(2)	2.403(7)
W–S′	2.422(6)	W–Cl(3)	2.396(6)
S–C(11)	1.76(2)	W–Cl(4)	2.383(5)
(*b*) W–bridge–W angles			
W–S–W′	62.6(1)	W–Cl(1)–W′	62.2(2)
(*c*) Bridge–W–bridge angles			
S–W–Cl(1)	96.0(1)	S–W–S′	94.6(2)
S′–W–Cl(1)	96.1(1)		
(*d*) Terminal–W–terminal angles			
Cl(2)–W–Cl(3)	87.1(2)	Cl(3)–W–Cl(4)	90.6(2)
Cl(2)–W–Cl(4)	90.5(2)		
(*e*) Bridge–W–terminal angles			
S–W–Cl(2)	90.5(2)	S′–W–Cl(4)	86.2(2)
S–W–Cl(3)	174.9(2)	Cl(1)–W–Cl(2)	87.1(2)
S–W–Cl(4)	84.8(2)	Cl(1)–W–Cl(3)	88.4(2)
S′–W–Cl(2)	173.7(2)	Cl(1)–W–Cl(4)	177.4(2)
S′–W–Cl(3)	87.6(2)		
(*f*) W–S–C angles			
W–S–C(11)	118.6(7)	W′–S–C(11)	116.4(8)

collection. Extended storage resulted in a complete breakdown of the crystal lattice. Although the standards measured during data collection showed no deterioration of the crystal, it is clear from the e.s.d.s on the cell parameters that the data crystal was already partially decomposed.

In the final cycle of refinement, the maximum shift-to-error ratio was 0.6 and the standard deviation in an observation of unit weight was 0.85. Secondary extinction could not be successfully refined. The model converged with agreement factors of $R = \Sigma(||F_o| - |F_c||)/\Sigma|F_o| = 0.072$ and $R' = [\Sigma w(|F_o| - |F_c|)^2/\Sigma w|F_o|^2]^{\frac{1}{2}} = 0.096$ (3 327 unique data, 357 variables). The weighting scheme used was $w = [\sigma^2(F_o) + 0.0006\,F_o^2]^{-1}$, where $\sigma(F_o)$ was derived from counting statistics. The final difference-Fourier map showed significant electron density only in the immediate environment (<1 Å) of the W atoms.

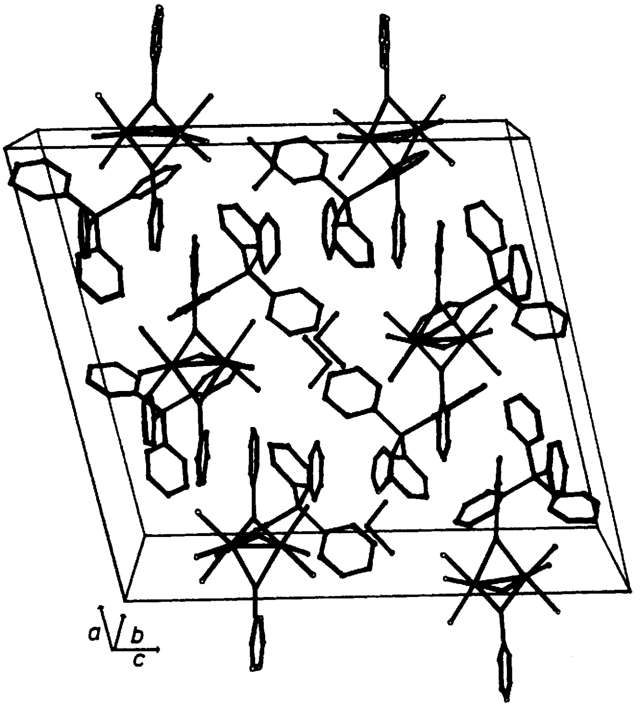

Figure 1. View of the unit-cell contents of $[AsPh_4]_2[Cl_3W(\mu\text{-}Cl)(\mu\text{-}SPh)_2WCl_3]\cdot 1.4CH_2Cl_2$ (1)

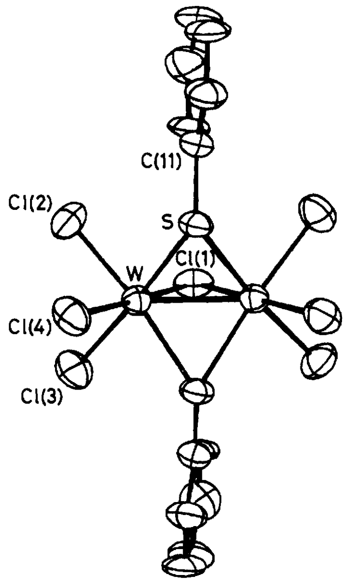

Figure 2. ORTEP view of the anion $[Cl_3W(\mu\text{-}Cl)(\mu\text{-}SPh)_2WCl_3]^{2-}$ showing the atomic numbering scheme

Table 1 summarizes the positional parameters of the non-hydrogen atoms of the anion of (1), and important bond lengths and bond angles for the $[Cl_3W(\mu\text{-}Cl)(\mu\text{-}SPh)_2WCl_3]^{2-}$ anion are listed in Table 2. A view of the unit-cell contents of (1) is shown in Figure 1, while two different views of the $[Cl_3W(\mu\text{-}Cl)(\mu\text{-}SPh)_2WCl_3]^{2-}$ anion are given in Figures 2 and 3.

E.S.R. Studies.—Electron spin resonance spectra of (1) as a powdered solid at 77 and 298 K and as a solution in CH_2Cl_2

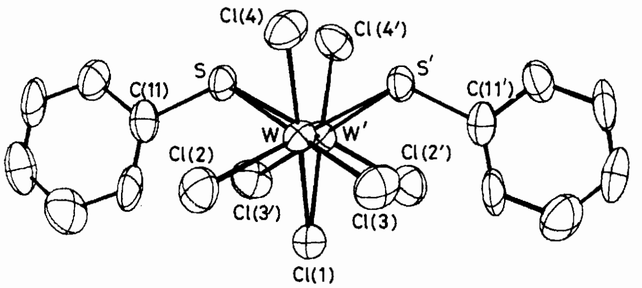

Figure 3. Alternate view of the anion $[Cl_3W(\mu\text{-}Cl)(\mu\text{-}SPh)_2WCl_3]^{2-}$ (approximately parallel to the tungsten–tungsten vector), illustrating the equatorial–equatorial disposition of the phenyl groups of the bridging thiolate ligands

at 77 K were obtained at *X*-band frequencies on a Varian E-112 spectrometer system. Variable temperature was achieved using an Oxford Instruments ESR 9 continuous-flow cryostat and a Harwell DT temperature controller.

Results and Discussion

Synthetic and Mechanistic Considerations.—Previous work in our laboratory has shown that by replacement of Cl by SR in the co-ordination sphere of tungsten complexes using the reagents $SiMe_3(SR)$, a variety of new metal–metal bonded dimeric compounds can be prepared.[4,5,19–22] The degradation of the initial product, $[WCl_3(SR)(SMe_2)_2]$, produced in the equimolar reaction between $[WCl_4(SMe_2)_2]$ and $SiMe_3(SR)$ has been shown thus far to occur either by reductive elimination of R_2S_2 or by loss of RCl, and that the degradation process is governed by the nature of the R group.[4,5,19–22] For cases where R = Ph, only the reductive elimination pathway has been observed in our studies. Thus it seemed likely that, by the treatment of $[WCl_4(SMe_2)_2]$ with $SiMe_3(SPh)$, lower oxidation state co-ordinatively unsaturated tungsten species would be generated, which in turn would be likely to dimerize or oligomerize. In the present case, the reaction apparently occurs as shown in equations (i) and (ii). A major product

$$[WCl_4(SMe_2)_2] + SiMe_3(SPh) \xrightarrow{CH_2Cl_2} [WCl_3(SPh)(SMe_2)_2] + SiMe_3Cl \quad \text{(i)}$$

$$n\ [WCl_3(SPh)(SMe_2)_2] \xrightarrow[\text{elimination of } Ph_2S_2]{\text{spontaneous reductive}} \text{products} \quad \text{(ii)}$$

from this reaction has been identified as $[(Me_2S)Cl_2W(\mu\text{-}Cl)(\mu\text{-}SPh)_2WCl_2(SMe_2)]$ (3). Analytical and spectroscopic data support this formulation, and the reaction of (3) with 2 mol equiv. of Cl^- has been shown to liberate 2 mol equiv. of SMe_2 with the concomitant formation of the anion $[Cl_3W(\mu\text{-}Cl)(\mu\text{-}SPh)_2WCl_3]^{2-}$, equation (iii). The tetraphenylphosphonium salt of the chloroanionic derivative of (3), $[PPh_4]_2[Cl_3W(\mu\text{-}Cl)(\mu\text{-}SPh)_2WCl_3]\cdot CH_2Cl_2$, can also be prepared in a similar fashion.[23]

$$\begin{array}{l} [(Me_2S)Cl_2W(\mu\text{-}Cl)(\mu\text{-}SPh)_2WCl_2(SMe_2)] + 2\ AsPh_4Cl \\ \qquad\qquad (3) \\ \qquad\qquad \downarrow CH_2Cl_2 \\ [AsPh_4]_2[Cl_3W(\mu\text{-}Cl)(\mu\text{-}SPh)_2WCl_3]\cdot 1.4CH_2Cl_2 + \\ \qquad\qquad (1) \qquad\qquad\qquad\qquad 2\ SMe_2 \quad \text{(iii)} \end{array}$$

The 200-MHz ^1H n.m.r. spectrum of (3) (CD_2Cl_2, 270 K) exhibits a poorly defined multiplet consisting of broad, overlapping signals in the region δ 7.1—8.0 p.p.m., assignable to the μ-SPh groups, and a collection of singlets between δ 2.5 and 2.8 p.p.m. representative of non-magnetically equivalent terminally bound SMe_2 groups. A consideration of (3) reveals that this neutral compound possesses the potential to exist in a number of structural and configurational isomeric forms, depending on the relative positions of the terminal SMe_2 ligands and the orientations of the phenyl rings of the μ-SPh moieties. The complicated appearance of the ^1H n.m.r. spectrum of (3) therefore suggests that it does indeed exist as a mixture of stereochemical and structural isomers. In addition, the broadness and ill defined nature of the μ-SPh resonances is not unexpected in view of the fact that the complex possesses one unpaired electron, probably in an orbital that is confined predominantly in the bridging region. This effect is even more accentuated in the ^1H n.m.r. spectrum of (1) for which no signals at all could be observed for the μ-SPh protons.

Structure of $[AsPh_4]_2[Cl_3W(\mu\text{-}Cl)(\mu\text{-}SPh)_2WCl_3]\cdot 1.4CH_2Cl_2$ (1).—Compound (1) consists of discrete $[Cl_3W(\mu\text{-}Cl)(\mu\text{-}SPh)_2WCl_3]^{2-}$ anions, $[AsPh_4]^+$ cations, and CH_2Cl_2 solvate molecules as is evident in Figure 1. The dinuclear tungsten anions are arranged in the unit cell such that the metal–metal vectors lie almost parallel to the *c* axis. Figures 2 and 3 show that the $[Cl_3W(\mu\text{-}Cl)(\mu\text{-}SPh)_2WCl_3]^{2-}$ anion possesses the confacial bioctahedral framework that is common for M_2L_9 species.[14,24] The short metal–metal separation [W–W' 2.519(2) Å] and the acute angles subtended at the atoms which bridge the tungsten centres [W–Cl(1)–W' 62.2(2), W–S–W' 62.6(1)°] suggest that a strong tungsten–tungsten bond exists in the anion of (1).[14,24] If there were no metal–metal attraction, the angles subtended at the bridging atoms would be expected to be equal to or greater than 70.5°,[14,24] and interaction between the tungsten atoms in the $[Cl_3W(\mu\text{-}Cl)(\mu\text{-}SPh)_2WCl_3]^{2-}$ ion consequently makes these angles more acute than the ideal value. The existence of a W–W bond in the anion of (1) is further substantiated by the fact that the $(\mu\text{-}Cl)(\mu\text{-}SPh)_2$ bridging unit does not intrinsically impose any degree of structural compression on confacial bioctahedral complexes. For example, no metal–metal bond exists in the cation $[(Ph_3P)_2HIr(\mu\text{-}Cl)(\mu\text{-}SPh)_2IrH(PPh_3)_2]^+$ [Ir–Ir 3.377(1) Å, Ir–(μ-X)–Ir (average) *ca.* 87°][25,26] and only a very weak metal–metal interaction was observed in the cation $[(Et_2NCS_2)OMo(\mu\text{-}Cl)(\mu\text{-}SPh)_2MoO(S_2CNEt_2)]^+$ [Mo–Mo 2.822(2) Å, Mo–(μ-X)–Mo (average) 68.51(7)°].[27] For a $W^{III}/W^{IV}(d^3/d^2)$ system, a formal bond order of 2.5 is predicted, and the preceding discussion along with the data summarized in Table 3 support the assignment of a tungsten–tungsten bond of this magnitude in the $[Cl_3W(\mu\text{-}Cl)(\mu\text{-}SPh)_2WCl_3]^{2-}$ anion of (1).

The configuration adopted by the two thiolato-sulphur atoms in the $[Cl_3W(\mu\text{-}Cl)(\mu\text{-}SPh)_2WCl_3]^{2-}$ ion can be described as equatorial–equatorial (*ee*)[28] (Figure 3). On the basis of steric considerations, the *ee* isomer would be expected to be the most stable, and in fact, the *ee* configuration is most often observed in the solid state for bis(thiolato)-bridged confacial bioctahedral species.[20–22] Axial–equatorial (*ae*) and axial–axial (*aa*) isomers of this type of complex have, however, been structurally characterized.[20,25–27] In solution, stereoisomeric interconversion is possible, and this process can be conveniently monitored by variable-temperature ^1H n.m.r.[21,22] The anion of (1) may be capable of such dynamic behaviour in solution, but the absence of phenyl resonances due to the bridging SPh moieties in the ^1H n.m.r. spectrum of (1) precluded any direct observation of an isomeric interconversion for the $[Cl_3W(\mu\text{-}Cl)(\mu\text{-}SPh)_2WCl_3]^{2-}$ ion.

Table 3. Comparison of the structural parameters of selected dinuclear tungsten species possessing confacial bioctahedral frameworks

Species	Oxidation states of the metal centres	Length of W–W vector (Å)	Average W–(μ-X)–W angle (°)	Assigned metal–metal bond order	Ref.
$[Cl_3W(\mu\text{-}Cl)_3WCl_3]^{3-}$	d^3/d^3	2.41	58°	3	*a*
$[Cl_3W(\mu\text{-}H)(\mu\text{-}SMe_2)_2WCl_3]^-$	d^3/d^3	2.410(7)	61.1(8)	3	*b*
$[(Me_2S)Cl_2W(\mu\text{-}S)(\mu\text{-}SEt)_2WCl_2(SMe_2)]$	d^2/d^2	2.526(2)	63.7(2)	2	20
$[(C_4H_8S)Cl_2W(\mu\text{-}S)(\mu\text{-}SEt)_2WCl_2(SC_4H_8)]$	d^2/d^2	2.524(1)	63.50(8)	2	19
$[(Me_2S)Cl_2W(\mu\text{-}SEt)_3WCl_2(SMe_2)]$	d^3/d^2	2.505(1)	62.3(2)	2.5	4
$[Cl_3W(\mu\text{-}Cl)(\mu\text{-}SPh)_2WCl_3]^{2-}$	d^3/d^2	2.519(2)	62.3(2)	2.5	*c*

[a] W. H. Watson and J. Wazer, *Acta Crystallogr.*, 1958, **11**, 689. [b] P. M. Boorman, K. J. Moynihan, and K. A. Kerr, *J. Chem. Soc., Chem. Commun.*, 1981, 1286. [c] This work.

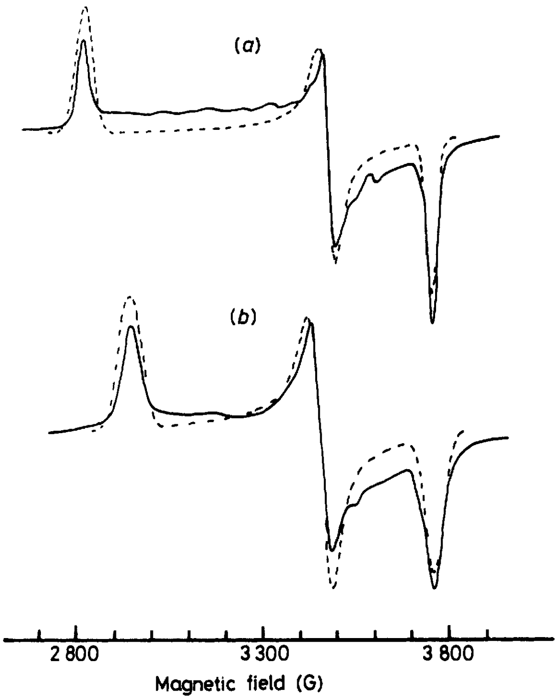

Figure 4. Experimental (——) and simulated (— — —) e.s.r. spectra of (1) at 77 K: (*a*) powdered sample, (*b*) frozen glass in CH_2Cl_2. 1 G = 10^{-4} T

Table 4. E.s.r. parameters * for $[AsPh_4]_2[Cl_3W(\mu\text{-}Cl)(\mu\text{-}SPh)_2WCl_3]\cdot 1.4CH_2Cl_2$

	Solid		Frozen solution in CH_2Cl_2
	Room temp.	77 K	(77 K)
g_1	2.311	2.343	2.238
g_2	1.893	1.896	1.907
g_3	1.747	1.752	1.754

* Estimated errors are ±0.002.

E.S.R. Studies.—The e.s.r. spectra of both powdered and frozen solution samples of (1) are those expected for a rhombic $S = \frac{1}{2}$ system, and can be simulated on this basis (Figure 4) with the parameters in Table 4. This interpretation was also confirmed by the *Q*-band powder spectrum of (1) at room temperature. We have been unable to observe any metal or ligand hyperfine structure in the spectra, and we have so far been unable to obtain crystals of sufficient size for single-crystal e.s.r. studies. The points of interest in these spectra are the very large anisotropy in the *g* values, and the observation that one of them is considerably greater than 2. With this large *g* value associated with the W–W direction,* we show below that qualitatively the pattern of *g* values is consistent with the approach of Summerville and Hoffmann [14] to the electronic structure of this type of compound.

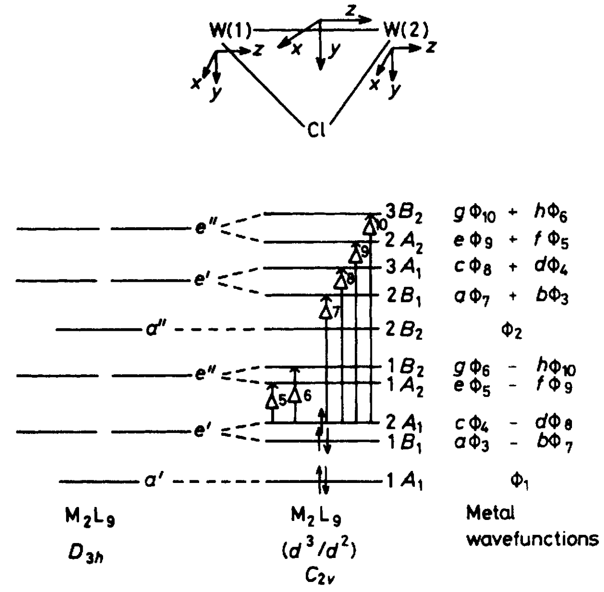

Figure 5. Axis systems and qualitative molecular orbital diagram for M_2L_9 species in C_{2v} point symmetry as a distortion from D_{3h} symmetry. Details for φ_i are given in the Appendix

Using the axis systems in Figure 5 and assuming C_{2v} symmetry, one possible ordering of the molecular orbitals associated with the bridging region is shown, along with their correlation to the higher symmetry (D_{3h}) M_2L_9 systems discussed by Summerville and Hoffmann.[14] The other possible ordering would involve inverting $1B_1$ and $2A_1$. General expressions for the *g* values [equations (iv)—(ix)] were derived, using the metal *d* orbitals only, by considering spin–orbit coupling as a simultaneous perturbation on the ground state and first

---

* Recent single-crystal e.s.r. studies on a related isostructural μ-SePh complex have substantiated this assignment (J. M. Ball, P. M. Boorman, F. E. Mabbs, K. J. Moynihan, and J. F. Richardson, unpublished work).

excited state, at δ, *i.e.* $(1A_1)^2(1B_1)^2(2A_1)^1$ or $(1A_1)^2(2A_1)^2(1B_1)^1$ as appropriate, plus second-order spin–orbit mixing with configurations arising from promotion of the unpaired electron in the ground state to empty orbitals at energies Δ_i. Although C_{2v} symmetry permits considerable mixing between the *d* orbitals we presume that this will be dominated by the mixings which are equivalent to hybrids, either directed towards, or having nodes directed towards, the bridging ligands.[14,29] Thus in the present compound the appropriate *d*-orbital mixing should be close to that on the metal centres, each with localised O_h symmetry; hence, for example, mixing between the A_1 orbitals involving d_{z^2} with the other A_1 orbitals is assumed to be unimportant.

For the $(1A_1)^2(1B_1)^2(2A_1)^1$ ground state, g_x, g_y, and g_z are given by equations (iv)—(vi); for the $(1A_1)^2(2A_1)^2(1B_1)^1$ ground state, the *g* values are given by equations (vii)—(ix),

$$g_z = 2.0023 - \frac{8N_1{}^2E}{\zeta} - \frac{2N_1{}^2\zeta(2bc + ad)^2}{\Delta_7} \qquad \text{(iv)}$$

$$g_x = 2.0023 - \frac{2N_1{}^2\zeta(hc - gd)^2}{\Delta_6} - \frac{2N_1{}^2\zeta\,(hd + gc)^2}{\Delta_{10}} \qquad \text{(v)}$$

$$g_y = 2.0023 - \frac{2N_1{}^2\zeta\,(ed - fc)^2}{\Delta_5} - \frac{2N_1{}^2\zeta\,(ec + df)^2}{\Delta_9} \qquad \text{(vi)}$$

$$g_z = 2.0023 - \frac{8N_1{}^2E}{\zeta} - \frac{2N_1{}^2\zeta(2ad + bc)^2}{\Delta_8} \qquad \text{(vii)}$$

$$g_x = 2.0023 - \frac{2N_1{}^2\zeta(eb - af)^2}{\Delta_5} - \frac{2N_1{}^2\zeta(ae + bf)^2}{\Delta_9} \qquad \text{(viii)}$$

$$g_y = 2.0023 - \frac{2N_1{}^2\zeta(gb - ah)^2}{\Delta_6} - \frac{2N_1{}^2\zeta(ag + bh)^2}{\Delta_{10}} \qquad \text{(ix)}$$

where E $(=\frac{1}{2}[\delta - \{\delta^2 + \zeta^2(2ac - bd)^2\}^{\frac{1}{2}}])$ and $N_1{}^2$ $(= [1 + 4E^2/\{\zeta^2(2ac - bd)^2\}]^{-1})$ are the energy and normalisation coefficient of the lowest doublet after first-order spin–orbit coupling, *a*—*h* are the metal *d*-orbital mixing coefficients (see Figure 5), Δ_i = energy separation between the ground state and the configuration obtained by promotion of the unpaired electron to an empty orbital (see Figure 5), and ζ = metal single-electron spin–orbit coupling constant.

In the limit of an idealised D_{3h} dimer, *g* values would be axially symmetric, with g_z tending to 4, as expected for an $(e')^3$ configuration. The lowering of the symmetry to approximately C_{2v} in (1) makes the *g* values rhombic, and raises the degeneracy of orbital doublets as indicated in Figure 5. This splitting of the $(e')^3$ configuration would depress g_z towards 2. However, for either possible ground state, *E* will be negative and hence g_z should remain greater than 2. The calculated *g* values are dependent on the energy separations δ, Δ_i, the metal spin–orbit coupling constant ζ, and on the *d*-orbital mixing coefficients. This makes it difficult quantitatively to interpret the *g* values at present. However, an approximate calculation can be made. As indicated above, the mixing coefficients may be approximated to those for an octahedron quantized with reference to a three-fold axis, *i.e.* from Figure 5, $a = c = e = g = \sqrt{\frac{2}{3}}$ and $b = d = f = h = -\sqrt{\frac{1}{3}}$. With a lower limit on Δ_i equal to the lowest energy band observed in the absorption spectrum, ζ = 1 800 cm^{-1} (the free-ion value for W^{III} [30]) and $\delta = 3\zeta$, we calculate $g_z = 2.28$ and because of these assumptions then $g_x = g_y = 1.82$. These calculated values are sufficiently close to the observed g_1 and the mean of g_2 and g_3 to indicate that the extension of the Summerville and Hoffmann [14] model to the present mixed oxidation state dimer gives a satisfactory qualitative account of its electronic structure.

Appendix

Symmetry-adapted *d*-electron wavefunctions used in the e.s.r. analysis. See Figure 5.

$$\varphi_1 = \frac{1}{\sqrt{2}}[d_{z^2}(1) + d_{z^2}(2)] \qquad A_1$$

$$\varphi_2 = \frac{1}{\sqrt{2}}[d_{z^2}(1) - d_{z^2}(2)] \qquad B_2$$

$$\varphi_3 = \frac{1}{\sqrt{2}}[d_{xy}(1) + d_{xy}(2)] \qquad B_1$$

$$\varphi_4 = \frac{1}{\sqrt{2}}[d_{x^2-y^2}(1) + d_{x^2-y^2}(2)] \qquad A_1$$

$$\varphi_5 = \frac{1}{\sqrt{2}}[d_{xy}(1) - d_{xy}(2)] \qquad A_2$$

$$\varphi_6 = \frac{1}{\sqrt{2}}[d_{x^2-y^2}(1) - d_{x^2-y^2}(2)] \qquad B_2$$

$$\varphi_7 = \frac{1}{\sqrt{2}}[d_{xz}(1) - d_{xz}(2)] \qquad B_1$$

$$\varphi_8 = \frac{1}{\sqrt{2}}[d_{yz}(1) - d_{yz}(2)] \qquad A_1$$

$$\varphi_9 = \frac{1}{\sqrt{2}}[d_{xz}(1) + d_{xz}(2)] \qquad A_2$$

$$\varphi_{10} = \frac{1}{\sqrt{2}}[d_{yz}(1) + d_{yz}(2)] \qquad B_2$$

Acknowledgements

We thank the Natural Sciences and Engineering Research Council of Canada for financial support (to P. M. B., J. M. B., and K. J. M.) and Dr. K. Ann Kerr for the use of the diffractometer.

References

1 See, for example, F. A. Cotton and G. Wilkinson, ' Advanced Inorganic Chemistry,' 4th edn., Wiley, New York, 1980.

2 R. E. McCarley, in ' Mixed-Valence Compounds,' ed. D. B. Brown, N.A.T.O. ASI Ser. C, D. Reidel, Dordrecht, Holland, 1980, vol. 58, p. 337.

3 J. L. Templeton, R. A. Jacobson, and R. E. McCarley, *Inorg. Chem.*, 1977, **16**, 3320.

4 P. M. Boorman, V. D. Patel, K. A. Kerr, P. W. Codding, and P. Van Roey, *Inorg. Chem.*, 1980, **19**, 3508.

5 V. D. Patel, Ph.D. Thesis, University of Calgary, 1981.

6 F. A. Cotton and E. Pedersen, *Inorg. Chem.*, 1975, **14**, 383.

7 F. A. Cotton and E. Pedersen, *Inorg. Chem.*, 1975, **14**, 388.

8 F. A. Cotton, B. A. Frenz, E. Pedersen, and T. R. Webb, *Inorg. Chem.*, 1975, **14**, 391.

9 F. A. Cotton and E. Pedersen, *Inorg. Chem.*, 1975, **14**, 399.

10 F. A. Cotton and E. Pedersen, *J. Am. Chem. Soc.*, 1975, **97**, 303.

11 G. A. Heath, G. Hefter, D. R. Robertson, W. J. Sime, and T. A. Stephenson, *J. Organomet. Chem.*, 1978, **152**, C1.

12 G. A. Heath, A. J. Lindsay, T. A. Stephenson, and D. K. Vattis, *J. Organomet. Chem.*, 1982, **233**, 353.

13 M. B. Robin and P. Day, *Adv. Inorg. Chem. Radiochem.*, 1967, **10**, 247.

14 R. H. Summerville and R. Hoffmann, *J. Am. Chem. Soc.*, 1979, **101**, 3821.

15 P. M. Boorman, T. Chivers, and K. N. Mahadev, *Can. J. Chem.*, 1975, **53**, 383; M. A. Schaefer King and R. E. McCarley, *Inorg. Chem.*, 1973, **12**, 1972.

16 E. W. Abel, *J. Chem. Soc.*, 1960, 4406.

17 D. T. Cromer and J. B. Mann, *Acta Crystallogr., Sect. A*, 1968, **24**, 321.

18 'International Tables for *X*-Ray Crystallography,' Kynoch Press, Birmingham, 1974, vol. 4, p. 149.

19 P. M. Boorman, K. A. Kerr, and V. D. Patel, *J. Chem. Soc., Dalton Trans.*, 1981, 506.

20 P. M. Boorman, P. W. Codding, K. A. Kerr, K. J. Moynihan, and V. D. Patel, *Can. J. Chem.*, 1982, **60**, 1333.

21 V. D. Patel and P. M. Boorman, *Can. J. Chem.*, 1982, **60**, 1339.

22 V. D. Patel, P. M. Boorman, K. A. Kerr, and K. J. Moynihan, *Inorg. Chem.*, 1982, **21**, 1383.

23 J. M. Ball, P. M. Boorman, K. J. Moynihan, and V. D. Patel, unpublished work.

24 F. A. Cotton and D. Ucko, *Inorg. Chim. Acta*, 1972, **6**, 161.

25 P. J. Roberts, G. Ferguson, and C. V. Senoff, *J. Organomet. Chem.*, 1975, **94**, C26.

26 P. J. Roberts and G. Ferguson, *Acta Crystallogr., Sect. B*, 1976, **32**, 1513.

27 G. Bunzey, J. H. Enemark, J. I. Gelder, and K. Yamanouchi, *J. Less Common Met.*, 1977, **54**, 101.

28 G. Natile, L. Maresca, and G. Bor, *Inorg. Chim. Acta*, 1977, **23**, 37.

29 J. L. Templeton, W. C. Dorman, J. C. Clardy, and R. E. McCarley, *Inorg. Chem.*, 1978, **17**, 1263.

30 B. N. Figgis and J. Lewis, *Prog. Inorg. Chem.*, 1964, **6**, 37.

Received 2*nd March* 1983; *Paper* 3/334